



Research article

Propagation patterns of dromion and other solitons in nonlinear Phi-Four (ϕ^4) equation

Mohammed Aldandani^{1,*}, Abdulhadi A. Altherwi^{2,*} and Mastoor M. Abushaega²

¹ Mathematics Department, College of Science, Jouf University, P. O. Box 2014, Sakaka, Kingdom of Saudi Arabia

² Department of Industrial Engineering, College of Engineering and Computer Science Jazan University, Jazan, Kingdom of Saudi Arabia

* **Correspondence:** Email: maldandani@ju.edu.sa, aaaltherwi@jazanu.edu.sa.

Abstract: The Phi-Four (also embodied as ϕ^4) equation (PFE) is one of the most significant models in nonlinear physics, that emerges in particle physics, condensed matter physics and cosmic theory. In this study, propagating soliton solutions for the PFE were obtained by employing the extended direct algebraic method (EDAM). This transformational method reformulated the model into an assortment of nonlinear algebraic equations using a series-form solution. These equations were then solved with the aid of Maple software, producing a large number of soliton solutions. New families of soliton solutions, including exponential, rational, hyperbolic, and trigonometric functions, are included in these solutions. Using 3D, 2D, and contour graphs, the shape, amplitude, and propagation behaviour of some solitons were visualized which revealed the existence of kink, shock, bright-dark, hump, lump-type, dromion, and periodic solitons in the context of PFE. The study was groundbreaking as it extended the suggested strategy to the PFE that was being aimed at, yielding a significant amount of soliton wave solutions while providing new insights into the behavioral characteristics of soliton. This approach surpassed previous approaches by offering a systematic approach to solving nonlinear problems in analogous challenging situations. Furthermore, the results also showed that the suggested method worked well for building families of propagating soliton solutions for intricate models such as the PFE.

Keywords: Phi-Four equation; nonlinear partial differential equation; extended direct algebraic method; nonlinear physics; solitons solutions; wave transformation

Mathematics Subject Classification: 34G20, 35A20, 35A22, 35R11

1. Introduction

In recent times, nonlinear partial differential equations (NPDEs) have gained significant prominence as fundamental research areas. This is especially true for the identification of novel features of complex phenomena across various fields, including particle, optical, nuclear, biological, and atomic physics [1–4]. Consequently, a multitude of nonlinear models have been created to illustrate diverse engineering, physics, and natural phenomena [5–7]. Because of the importance of these models and their many applications, a large number of mathematicians have devised a variety of techniques and approaches to investigate analytical, numerical, and semi-analytical solutions. Spline methods [8], the Adomian decomposition method [9], finite difference method [10], the variational iteration method [11], the (G'/G) -expansion method [12], the sine-cosine expansion method [13], the Riccati expansion method [14], the tanh-expansion method [15], the sech-tanh expansion method [16], the modified simple equation method [17] and many other tools [18–20] are devolved by academics to address such nonlinear models.

The significance of looking into methods to solve NPDEs and is essential to understanding the actions of numerous elements in a range of scientific areas [21]. Since soliton solutions to NPDEs provide greater breadth and detail than traditional solutions, they continue to be important from an academic standpoint. A single, self-sustaining wave packet that travels through a medium without changing its form or speed is known as a soliton. Their inherent stability and durability make them valuable in numerous technical and scientific domains. For nonlinear systems, they offer efficient information transfer and long-distance coherence maintenance. Mathematicians have developed robust approaches in pursuit of new soliton solution results. Among such notable approaches are the Sin-Gordon method [22], Khater methods [23], Poincaré-Lighthill-Kuo method [24], (G'/G) -expansion method [25, 26], exp-function method [27], Riccati-Bernoulli Sub-ordinary differential equation [28], Kudryashov method [29], sub-equation method [30], Sardar sub-equation method [31], Hirota's bilinear method [32] and extended direct algebraic method [33–36], among others.

In this study, a reliable and efficient analytical approach namely, EDAM, is used to address the nonlinear Phi-Four equation (PFE) in order to find and examine a new plethora of propagating soliton solutions for the model under consideration. The theoretical wave instruction that in the wave-mechanical principle corresponds to a moving elementary particle (as an electron rather than a proton) strikes together with such or offers the particle definitive suspense properties (as thrusting then diffraction) is defined as de Broglie waves. The analytical solutions characterize the physical and dynamical behavior of the relativistic electrons, the spineless relativistic composite particles, and these particles. On the other hand, the relativistic might describe the permanence of transfer at an absolute velocity, meaning that there is even a significant exchange of attributes (like a lot of mass). There is a relativistic electron, if the theory of relativity is correct. The following system contains the nonlinear PFEs [37]:

$$\begin{aligned} (w^\pm)_t - \omega(w^\pm)_{xx} - w + w^\pm &= 0, \\ (w^\pm)_t - \omega(w^\pm)_{xx} - w^m + w^\pm &= 0, \end{aligned} \tag{1.1}$$

where ω is an arbitrary constant and $w = w(x, t)$ provides the physical characteristics of the relativistic electrons, spineless relativistic composite particles, and deBroglie waves. Two fundamental solutions of Eq (1.1) at high velocities of the exact solution are kink and anti-kind solutions. The following

formula is used in a previous published study to formulate these solutions mathematically [38]:

$$w(x, t) = \pm \tanh\left(\frac{\sqrt{2}}{2\sqrt{1-\omega^2}}(x - \omega t)\right). \quad (1.2)$$

The PFE with $m = 1$ is examined in this research derive, so, the nonlinear PFE is provided as follows [39–42]:

$$w_{tt} - w_{xx} + \alpha^2 w + \beta w^3 = 0, \quad (1.3)$$

where arbitrary constants α and β are to be assessed thereafter. Prior to this research work, several academics have addressed PFE with different analytical and numerical techniques. For instance, Khater et al. in [39] investigated the semi-analytical and analytical solutions of PFE by the means of the modified $\left(\frac{\Psi'}{\Psi}\right)$ -expansion method, Adomian decomposition method and sech-tanh expansion method. Similarly, the generalized Kudryashov method was used by Mahmud et al. to construct traveling wave solutions for PFE [43]. Gao et al. addressed PFE using q-homotopy analysis transform method to acquire numerical solutions for it [37]. Finally, Younis et al. used the modified simple equation method to solve the PFE analytically for the construction of many traveling wave solutions [44]. However, the main aim of this research derive is to construct and analyze new plethora of soliton and other traveling wave solutions for PFE. This transformational method reformulates the model into a collection of nonlinear algebraic equations using a series-form solution. These equations are then solved with the aid of Maple software, producing a large number of soliton solutions. New families of functions, including exponential, rational, hyperbolic, and trigonometric functions, are included in these solutions. Using 3D, 2D, and contour graphs, the shape, amplitude, and propagation pattern of some solitons are visualized. Kink, shock, bright-dark, hump, lump-type, dromion, and periodic solitons are clearly seen. The study is revolutionary since it applies the recommended technique to the PFE that is being targeted, producing a sizable number of soliton wave solutions and offering fresh perspectives on the behaviors of soliton. This method outperforms earlier methods by providing a methodical way to solve nonlinear problems in comparable difficult scenarios. Moreover, the outcomes demonstrate that the proposed approach is effective in constructing families of transmitting soliton solutions for complex models like the PFE [45–51].

The remaining pattern of this paper is as follows: The working methodology of EDAM is described in Section 2, the nonlinear PFE's soliton solutions with the EDAM are constructed in Section 3, and Section 4 is illustrated with several graphs and a discussion over the propagation of graphed solitons. Our paper's Conclusion section provides an overview of all the outcomes we were able to gather.

2. The operational procedure of EDAM

This section's goal is to present a general description of the EDAM. Look into the NPDE in the following form:

$$E(\psi, \partial_t \psi, \partial_{v_1} \psi, \partial_{v_2} \psi, \psi \partial_{v_1} \psi, \dots) = 0, \quad (2.1)$$

where $\psi = \psi(t, v_1, v_2, v_3, \dots, v_n)$. In order to solve Eq (2.1), the following steps are followed:

Step 1. First, we perform a variable transformation on the Eq (2.1) in the form $\psi(t, v_1, v_2, v_3, \dots, v_n)$

$= \Psi(\varphi)$, where φ is a function of $t, v_1, v_2, v_3, \dots, v_n$ and can take several forms. This transformation turns (2.1) into a nonlinear ordinary differential equation (NODE), which has the following structure:

$$F(\Psi, \Psi', \Psi\Psi', \dots) = 0, \quad \text{where} \quad \Psi' = \frac{d\Psi}{d\varphi}. \quad (2.2)$$

On rare occasions, Eq (2.2) can be integrated once or more to make it suitable for the homogenous balance principle.

Step 2. Next, we assume that (2.2) has the following closed form solution:

$$\Psi(\varphi) = \sum_{i=-\tau}^{\tau} s_i(\rho(\varphi))^i. \quad (2.3)$$

Here, s_i 's denotes parameters that require estimation. Moreover, another NODE of the following type is satisfied by $\rho(\varphi)$:

$$\rho'(\varphi) = k + l\rho(\varphi) + m(\rho(\varphi))^2, \quad (2.4)$$

where k, l, m are constants.

Step 3. Upon searching for the homogeneous balance between the largest order derivative in Eq (2.2) and the prevailing nonlinear element, we find a positive integer τ (shown in Eq (2.3)).

Step 4. Then, we substitute (2.3) in (2.2) or in the equation that results from integrating (2.2), and lastly, we combine all of the terms of $\rho(\varphi)$ in the same order to get a polynomial in $\rho(\varphi)$. If all the coefficients of the resultant polynomial are set to zero, a system of algebraic equations for s_i 's and additional parameters is obtained.

Step 5. After that, this system of nonlinear algebraic equations is solved using Maple.

Step 6. Equation (2.3) and the associated solution $\rho(\varphi)$ from Eq (2.4), together with the unknown parameters, are used to get the traveling wave solutions to Eq (2.1). The families of traveling wave solutions that are displayed below can be created by applying the general solution of Eq (2.4).

Family 1. For $\Omega < 0$ and $m \neq 0$:

$$\rho_1(\varphi) = -\frac{l}{2m} + \frac{\sqrt{-\Omega} \tan\left(\frac{1}{2} \sqrt{-\Omega}\varphi\right)}{2m},$$

$$\rho_2(\varphi) = -\frac{l}{2m} - \frac{\sqrt{-\Omega} \cot\left(\frac{1}{2} \sqrt{-\Omega}\varphi\right)}{2m},$$

$$\rho_3(\varphi) = -\frac{l}{2m} + \frac{\sqrt{-\Omega} \left(\tan\left(\sqrt{-\Omega}\varphi\right) + \left(\sec\left(\sqrt{-\Omega}\varphi\right)\right) \right)}{2m},$$

$$\rho_4(\varphi) = -\frac{l}{2m} - \frac{\sqrt{-\Omega} \left(\cot\left(\sqrt{-\Omega}\varphi\right) + \left(\csc\left(\sqrt{-\Omega}\varphi\right)\right) \right)}{2m},$$

and

$$\rho_5(\varphi) = -\frac{l}{2m} + \frac{\sqrt{-\Omega} \left(\tan\left(\frac{1}{4} \sqrt{-\Omega}\varphi\right) - \cot\left(\frac{1}{4} \sqrt{-\Omega}\varphi\right) \right)}{4m}.$$

Family 2. For $\Omega > 0$ and $m \neq 0$:

$$\rho_6(\varphi) = -\frac{l}{2m} - \frac{\sqrt{\Omega} \tanh\left(\frac{1}{2} \sqrt{\Omega}\varphi\right)}{2m},$$

$$\rho_7(\varphi) = -\frac{l}{2m} - \frac{\sqrt{\Omega} \coth\left(\frac{1}{2} \sqrt{\Omega}\varphi\right)}{2m},$$

$$\rho_8(\varphi) = -\frac{l}{2m} - \frac{\sqrt{\Omega} \left(\tanh\left(\sqrt{\Omega}\varphi\right) + i \left(\operatorname{sech}\left(\sqrt{\Omega}\varphi\right) \right) \right)}{2m},$$

$$\rho_9(\varphi) = -\frac{l}{2m} - \frac{\sqrt{\Omega} \left(\coth\left(\sqrt{\Omega}\varphi\right) + \left(\operatorname{csch}\left(\sqrt{\Omega}\varphi\right) \right) \right)}{2m},$$

and

$$\rho_{10}(\varphi) = -\frac{l}{2m} - \frac{\sqrt{\Omega} \left(\tanh\left(\frac{1}{4} \sqrt{\Omega}\varphi\right) - \coth\left(\frac{1}{4} \sqrt{\Omega}\varphi\right) \right)}{4m}.$$

Family 3. For $km > 0$ and $l = 0$:

$$\rho_{11}(\varphi) = \sqrt{\frac{k}{m}} \tan\left(\sqrt{km}\varphi\right),$$

$$\rho_{12}(\varphi) = -\sqrt{\frac{k}{m}} \cot\left(\sqrt{km}\varphi\right),$$

$$\rho_{13}(\varphi) = \sqrt{\frac{k}{m}} \left(\tan\left(2\sqrt{km}\varphi\right) + \left(\sec\left(2\sqrt{km}\varphi\right) \right) \right),$$

$$\rho_{14}(\varphi) = -\sqrt{\frac{k}{m}} \left(\cot\left(2\sqrt{km}\varphi\right) + \left(\operatorname{csc}\left(2\sqrt{km}\varphi\right) \right) \right),$$

and

$$\rho_{15}(\varphi) = \frac{1}{2} \sqrt{\frac{k}{m}} \left(\tan\left(\frac{1}{2} \sqrt{km}\varphi\right) - \cot\left(\frac{1}{2} \sqrt{km}\varphi\right) \right).$$

Family 4. For $km < 0$ and $l = 0$:

$$\rho_{16}(\varphi) = -\sqrt{-\frac{k}{m}} \tanh\left(\sqrt{-km}\varphi\right),$$

$$\rho_{17}(\varphi) = -\sqrt{-\frac{k}{m}} \coth\left(\sqrt{-km}\varphi\right),$$

$$\rho_{18}(\varphi) = -\sqrt{-\frac{k}{m}} \left(\tanh\left(2\sqrt{-km}\varphi\right) + \left(\operatorname{isech}\left(2\sqrt{-km}\varphi\right) \right) \right),$$

$$\rho_{19}(\varphi) = -\sqrt{-\frac{k}{m}} \left(\coth\left(2\sqrt{-km}\varphi\right) + \left(\operatorname{csch}\left(2\sqrt{-km}\varphi\right) \right) \right),$$

and

$$\rho_{20}(\varphi) = -\frac{1}{2} \sqrt{-\frac{k}{m}} \left(\tanh\left(\frac{1}{2} \sqrt{km}\varphi\right) + \coth\left(\frac{1}{2} \sqrt{-km}\varphi\right) \right).$$

Family 5. For $m = k$ and $l = 0$:

$$\rho_{21}(\varphi) = \tan(k\varphi),$$

$$\rho_{22}(\varphi) = -\cot(k\varphi),$$

$$\rho_{23}(\varphi) = \tan(2k\varphi) + (\sec(2k\varphi)),$$

$$\rho_{24}(\varphi) = -\cot(2k\varphi) + (\csc(2k\varphi)),$$

and

$$\rho_{25}(\varphi) = \frac{1}{2} \tan\left(\frac{1}{2}k\varphi\right) - \frac{1}{2} \cot\left(\frac{1}{2}k\varphi\right).$$

Family 6. For $m = -k$ and $l = 0$:

$$\rho_{26}(\varphi) = -\tanh(k\varphi),$$

$$\rho_{27}(\varphi) = -\coth(k\varphi),$$

$$\rho_{28}(\varphi) = -\tanh(2k\varphi) + (\operatorname{isech}(2k\varphi)),$$

$$\rho_{29}(\varphi) = -\coth(2k\varphi) + (\operatorname{csch}(2k\varphi)),$$

and

$$\rho_{30}(\varphi) = -\frac{1}{2} \tanh\left(\frac{1}{2}k\varphi\right) - \frac{1}{2} \coth\left(\frac{1}{2}k\varphi\right).$$

Family 7. For $\Omega = 0$:

$$\rho_{31}(\varphi) = -2 \frac{k(l\varphi + 2)}{l^2\varphi}.$$

Family 8. For $m = 0$, $l = \kappa$ and $k = n\kappa$ (with $n \neq 0$):

$$\rho_{32}(\varphi) = e^{k\varphi} - n.$$

Family 9. For $l = m = 0$:

$$\rho_{33}(\varphi) = k\varphi.$$

Family 10. For $l = k = 0$:

$$\rho_{34}(\varphi) = -\frac{1}{m\varphi}.$$

Family 11. For $l \neq 0$, $m \neq 0$ and $k = 0$:

$$\rho_{35}(\varphi) = -\frac{l}{m(\cosh(l\varphi) - \sinh(l\varphi) + 1)},$$

and

$$\rho_{36}(\varphi) = -\frac{l(\cosh(l\varphi) + \sinh(l\varphi))}{m(\cosh(l\varphi) + \sinh(l\varphi) + 1)}.$$

Family 12. For $l = \kappa$, $m = n\kappa$ (with $n \neq 0$), and $k = 0$:

$$\rho_{37}(\varphi) = \frac{e^{k\varphi}}{1 - se^{k\varphi}}.$$

In the above solutions, $\Omega = l^2 - 4km$.

3. Construction of soliton solutions for PFE

In this part, we apply the proposed EDAM to derive soliton solutions for the chosen PFE given in (1.3). To begin, we define the following wave transformation concept:

$$w(x, t) = W(\varphi), \quad \text{where } \varphi = x + \omega t, \quad (3.1)$$

where the wave's velocity is indicated by ω . Performing the aforementioned wave transformation to Eq (1.3), an NPDE, yields the resulting NODE:

$$(\omega^2 - 1)W''(\varphi) + \alpha^2 W(\varphi) + \beta W^3(\varphi) = 0. \quad (3.2)$$

Establishing the homogeneous balance principle between $W''(\varphi)$ and $W^3(\varphi)$ in (3.1) suggests $\tau = 1$. Plugging $\tau = 1$ in Eq (2.3) yields the subsequent series solution for Eq (3.1):

$$W(\varphi) = \sum_{i=-1}^1 s_i (\rho(\varphi))^i. \quad (3.3)$$

By inserting (3.2) into (3.1) and collecting each term with the identical orders of $\rho(\varphi)$, an expression in $\rho(\varphi)$ is produced. By equating the coefficients of the formula to zero, it can be simplified into a system of nonlinear algebraic equations. The ensuing three (1.3) types of solutions are obtained when using Maple to tackle the resulting problem:

Case 1.

$$s_0 = \frac{s_{-1}l}{2k}, \quad s_1 = 0, \quad s_{-1} = s_{-1}, \quad \alpha = \frac{1}{2} \sqrt{2\omega^2\Omega - 2\Omega}, \quad \beta = -2 \frac{k^2(\omega^2 - 1)}{s_{-1}^2}, \quad \omega = \omega. \quad (3.4)$$

Case 2.

$$s_0 = \frac{s_1l}{2m}, \quad s_1 = s_1, \quad s_{-1} = 0, \quad \alpha = \frac{1}{2} \sqrt{2\omega^2\Omega - 2\Omega}, \quad \beta = -2 \frac{m^2(\omega^2 - 1)}{s_1^2}, \quad \omega = \omega. \quad (3.5)$$

Case 3.

$$s_0 = s_0, \quad s_1 = s_1, \quad s_{-1} = s_{-1}, \quad \alpha = 0, \quad \beta = 0, \quad \omega = \pm 1. \quad (3.6)$$

By taking into account Case 1 and using Eqs (3.1) and (3.2) with the corresponding solution of (2.4), we produce the following plethora of soliton solutions for PFE stated in (1.3):

Family 1.1. For $\Omega < 0$ and $m \neq 0$:

$$w_{1,1}(t, x) = \frac{s_{-1}l}{2k} + s_{-1} \left(-\frac{l}{2m} + \frac{\sqrt{-\Omega} \tan\left(\frac{1}{2} \sqrt{-\Omega} \varphi\right)}{2m} \right)^{-1}, \quad (3.7)$$

$$w_{1,2}(t, x) = \frac{s_{-1}l}{2k} + s_{-1} \left(-\frac{l}{2m} - \frac{\sqrt{-\Omega} \cot\left(\frac{1}{2} \sqrt{-\Omega} \varphi\right)}{2m} \right)^{-1}, \quad (3.8)$$

$$w_{1,3}(t, x) = \frac{s_{-1}l}{2k} + s_{-1} \left(-\frac{l}{2m} + \frac{\sqrt{-\Omega} (\tan(\sqrt{-\Omega}\varphi) + \sec(\sqrt{-\Omega}\varphi))}{2m} \right)^{-1}, \quad (3.9)$$

$$w_{1,4}(t, x) = \frac{s_{-1}l}{2k} + s_{-1} \left(-\frac{l}{2m} - \frac{\sqrt{-\Omega} (\cot(\sqrt{-\Omega}\varphi) + \csc(\sqrt{-\Omega}\varphi))}{2m} \right)^{-1}, \quad (3.10)$$

$$w_{1,5}(t, x) = \frac{s_{-1}l}{2k} + s_{-1} \left(-\frac{l}{2m} + \frac{\sqrt{-\Omega} (\tan(\frac{1}{4}\sqrt{-\Omega}\varphi) - \cot(\frac{1}{4}\sqrt{-\Omega}\varphi))}{4m} \right)^{-1}. \quad (3.11)$$

Family 1.2. For $\Omega > 0$ and $m \neq 0$:

$$w_{1,6}(t, x) = \frac{s_{-1}l}{2k} + s_{-1} \left(-\frac{l}{2m} - \frac{\sqrt{\Omega} \tanh(\frac{1}{2}\sqrt{\Omega}\varphi)}{2m} \right)^{-1}, \quad (3.12)$$

$$w_{1,7}(t, x) = \frac{s_{-1}l}{2k} + s_{-1} \left(-\frac{l}{2m} - \frac{\sqrt{\Omega} \coth(\frac{1}{2}\sqrt{\Omega}\varphi)}{2m} \right)^{-1}, \quad (3.13)$$

$$w_{1,8}(t, x) = \frac{s_{-1}l}{2k} + s_{-1} \left(-\frac{l}{2m} - \frac{\sqrt{\Omega} (\tanh(\sqrt{\Omega}\varphi) + i \operatorname{sech}(\sqrt{\Omega}\varphi))}{2m} \right)^{-1}, \quad (3.14)$$

$$w_{1,9}(t, x) = \frac{s_{-1}l}{2k} + s_{-1} \left(-\frac{l}{2m} - \frac{\sqrt{\Omega} (\coth(\sqrt{\Omega}\varphi) + \operatorname{csch}(\sqrt{\Omega}\varphi))}{2m} \right)^{-1}, \quad (3.15)$$

$$w_{1,10}(t, x) = \frac{s_{-1}l}{2k} + s_{-1} \left(-\frac{l}{2m} - \frac{\sqrt{\Omega} (\tanh(\frac{1}{4}\sqrt{\Omega}\varphi) - \coth(\frac{1}{4}\sqrt{\Omega}\varphi))}{4m} \right)^{-1}. \quad (3.16)$$

Family 1.3. For $km > 0$ and $l = 0$:

$$w_{1,11}(t, x) = s_{-1} \sqrt{\frac{m}{k}} (\tan(\sqrt{mk}\varphi))^{-1}, \quad (3.17)$$

$$w_{1,12}(t, x) = -s_{-1} \sqrt{\frac{m}{k}} (\cot(\sqrt{mk}\varphi))^{-1}, \quad (3.18)$$

$$w_{1,13}(t, x) = s_{-1} \sqrt{\frac{m}{k}} (\tan(2\sqrt{mk}\varphi) + \sec(2\sqrt{mk}\varphi))^{-1}, \quad (3.19)$$

$$w_{1,14}(t, x) = -s_{-1} \sqrt{\frac{m}{k}} (\cot(2\sqrt{mk}\varphi) + \csc(2\sqrt{mk}\varphi))^{-1}, \quad (3.20)$$

$$w_{1,15}(t, x) = 2s_{-1} \sqrt{\frac{m}{k}} \left(\tan\left(\frac{1}{2}\sqrt{mk}\varphi\right) - \cot\left(\frac{1}{2}\sqrt{mpk}\varphi\right) \right)^{-1}. \quad (3.21)$$

Family 1.4. For $km < 0$ and $l = 0$:

$$w_{1,16}(t, x) = -s_{-1} \sqrt{-\frac{m}{k}} (\tanh(\sqrt{-mk}\varphi))^{-1}, \quad (3.22)$$

$$w_{1,17}(t, x) = -s_{-1} \sqrt{-\frac{m}{k}} \left(\coth \left(\sqrt{-km}\varphi \right) \right)^{-1}, \quad (3.23)$$

$$w_{1,18}(t, x) = -s_{-1} \sqrt{-\frac{m}{k}} \left(\tanh \left(2 \sqrt{-km}\varphi \right) + \left(\operatorname{sech} \left(2 \sqrt{-km}\varphi \right) \right) \right)^{-1}, \quad (3.24)$$

$$w_{1,19}(t, x) = -s_{-1} \sqrt{-\frac{m}{k}} \left(\coth \left(2 \sqrt{-km}\varphi \right) + \left(\operatorname{csch} \left(2 \sqrt{-km}\varphi \right) \right) \right)^{-1}, \quad (3.25)$$

$$w_{1,20}(t, x) = -2 s_{-1} \sqrt{-\frac{m}{k}} \left(\tanh \left(\frac{1}{2} \sqrt{-km}\varphi \right) + \coth \left(\frac{1}{2} \sqrt{-km}\varphi \right) \right)^{-1}. \quad (3.26)$$

Family 1.5. For $m = k$ and $l = 0$:

$$w_{1,21}(t, x) = \frac{s_{-1}}{\tan(m\varphi)}, \quad (3.27)$$

$$w_{1,22}(t, x) = -\frac{s_{-1}}{\cot(m\varphi)}, \quad (3.28)$$

$$w_{1,23}(t, x) = \frac{s_{-1}}{\tan(2m\varphi) + \sec(2m\varphi)}, \quad (3.29)$$

$$w_{1,24}(t, x) = \frac{s_{-1}}{-\cot(2m\varphi) + \csc(2m\varphi)}, \quad (3.30)$$

$$w_{1,25}(t, x) = \frac{s_{-1}}{\frac{1}{2} \tan\left(\frac{1}{2}m\varphi\right) - \frac{1}{2} \cot\left(\frac{1}{2}m\varphi\right)}. \quad (3.31)$$

Family 1.6. For $m = -k$ and $l = 0$:

$$w_{1,26}(t, x) = -\frac{s_{-1}}{\tanh(k\varphi)}, \quad (3.32)$$

$$w_{1,27}(t, x) = -\frac{s_{-1}}{\coth(k\varphi)}, \quad (3.33)$$

$$w_{1,28}(t, x) = \frac{s_{-1}}{-\tanh(2k\varphi) + i \operatorname{sech}(2k\varphi)}, \quad (3.34)$$

$$w_{1,29}(t, x) = \frac{s_{-1}}{-\coth(2k\varphi) + \operatorname{csch}(2k\varphi)}, \quad (3.35)$$

$$w_{1,30}(t, x) = \frac{s_{-1}}{-\frac{1}{2} \tanh\left(\frac{1}{2}k\varphi\right) - \frac{1}{2} \coth\left(\frac{1}{2}k\varphi\right)}. \quad (3.36)$$

Family 1.7. For $\Omega = 0$:

$$w_{1,31}(t, x) = \frac{1}{2} \frac{s_{-1}l}{k} - \frac{1}{2} \frac{s_{-1}k\varphi}{l\varphi + 2}. \quad (3.37)$$

Family 1.8. For $m = 0$, $l = \kappa$ and $k = n\kappa$ (with $n \neq 0$):

$$w_{1,32}(t, x) = \frac{1}{2} \frac{s_{-1}}{n} + \frac{s_{-1}}{e^{\kappa\varphi} - n}. \quad (3.38)$$

Family 1.9. For $l = m = 0$:

$$w_{1,33}(t, x) = \frac{s_{-1}}{k\varphi}. \quad (3.39)$$

In the above solutions, $\varphi = x + \omega t$.

By taking into account Case 2 and using Eqs (3.1) and (3.2) with the corresponding solution of (2.4), we produce the following plethora of soliton solutions for PFE stated in (1.3):

Family 2.1. For $\Omega < 0$ and $m \neq 0$:

$$w_{2,1}(t, x) = \frac{s_1 l}{2m} + s_1 \left(-\frac{l}{2m} + \frac{\sqrt{-\Omega} \tan\left(\frac{1}{2} \sqrt{-\Omega} \varphi\right)}{2m} \right), \quad (3.40)$$

$$w_{2,2}(t, x) = \frac{s_1 l}{2m} + s_1 \left(-\frac{l}{2m} - \frac{\sqrt{-\Omega} \cot\left(\frac{1}{2} \sqrt{-\Omega} \varphi\right)}{2m} \right), \quad (3.41)$$

$$w_{2,3}(t, x) = \frac{s_1 l}{2m} + s_1 \left(-\frac{l}{2m} + \frac{\sqrt{-\Omega} \left(\tan\left(\sqrt{-\Omega} \varphi\right) + \sec\left(\sqrt{-\Omega} \varphi\right) \right)}{2m} \right), \quad (3.42)$$

$$w_{2,4}(t, x) = \frac{s_1 l}{2m} + s_1 \left(-\frac{l}{2m} - \frac{\sqrt{-\Omega} \left(\cot\left(\sqrt{-\Omega} \varphi\right) + \csc\left(\sqrt{-\Omega} \varphi\right) \right)}{2m} \right), \quad (3.43)$$

$$w_{2,5}(t, x) = \frac{s_1 l}{2m} + s_1 \left(-\frac{l}{2m} + \frac{\sqrt{-\Omega} \left(\tan\left(\frac{1}{4} \sqrt{-\Omega} \varphi\right) - \cot\left(\frac{1}{4} \sqrt{-\Omega} \varphi\right) \right)}{4m} \right). \quad (3.44)$$

Family 2.2. For $\Omega > 0$ and $m \neq 0$:

$$w_{2,6}(t, x) = \frac{s_1 l}{2m} + s_1 \left(-\frac{l}{2m} - \frac{\sqrt{\Omega} \tanh\left(\frac{1}{2} \sqrt{\Omega} \varphi\right)}{2m} \right), \quad (3.45)$$

$$w_{2,7}(t, x) = \frac{s_1 l}{2m} + s_1 \left(-\frac{l}{2m} - \frac{\sqrt{\Omega} \coth\left(\frac{1}{2} \sqrt{\Omega} \varphi\right)}{2m} \right), \quad (3.46)$$

$$w_{2,8}(t, x) = \frac{s_1 l}{2m} + s_1 \left(\frac{l}{2m} - \frac{\sqrt{\Omega} \left(\tanh\left(\sqrt{\Omega} \varphi\right) + i \operatorname{sech}\left(\sqrt{\Omega} \varphi\right) \right)}{2m} \right), \quad (3.47)$$

$$w_{2,9}(t, x) = \frac{s_1 l}{2m} + s_1 \left(-\frac{l}{2m} - \frac{\sqrt{\Omega} \left(\coth\left(\sqrt{\Omega} \varphi\right) + \operatorname{csch}\left(\sqrt{\Omega} \varphi\right) \right)}{2m} \right), \quad (3.48)$$

$$w_{2,10}(t, x) = \frac{s_1 l}{2m} + s_1 \left(-\frac{l}{2m} - \frac{\sqrt{\Omega} \left(\tanh\left(\frac{1}{4} \sqrt{\Omega} \varphi\right) - \coth\left(\frac{1}{4} \sqrt{\Omega} \varphi\right) \right)}{4m} \right). \quad (3.49)$$

Family 2.3. For $km > 0$ and $l = 0$:

$$w_{2,11}(t, x) = s_1 \sqrt{\frac{k}{m}} \tan\left(\sqrt{mk} \varphi\right), \quad (3.50)$$

$$w_{2,12}(t, x) = -s_1 \sqrt{\frac{k}{m}} \cot(\sqrt{mk}\varphi), \quad (3.51)$$

$$w_{2,13}(t, x) = s_1 \sqrt{\frac{k}{m}} \left(\tan(2\sqrt{mk}\varphi) + \sec(2\sqrt{mk}\varphi) \right), \quad (3.52)$$

$$w_{2,14}(t, x) = s_1 \left(-\sqrt{\frac{k}{m}} \left(\cot(2\sqrt{mk}\varphi) + \csc(2\sqrt{mk}\varphi) \right) \right), \quad (3.53)$$

$$w_{2,15}(t, x) = \frac{1}{2} s_1 \sqrt{\frac{k}{m}} \left(\tan\left(\frac{1}{2}\sqrt{mk}\varphi\right) - \cot\left(\frac{1}{2}\sqrt{mk}\varphi\right) \right). \quad (3.54)$$

Family 2.4. For $km < 0$ and $l = 0$:

$$w_{2,16}(t, x) = -s_1 \sqrt{-\frac{k}{m}} \tanh(\sqrt{-mk}\varphi), \quad (3.55)$$

$$w_{2,17}(t, x) = -s_1 \sqrt{-\frac{k}{m}} \coth(\sqrt{-mk}\varphi), \quad (3.56)$$

$$w_{2,18}(t, x) = -s_1 \sqrt{-\frac{k}{m}} \left(\tanh(2\sqrt{-km}\varphi) + (\operatorname{isech}(2\sqrt{-km}\varphi)) \right), \quad (3.57)$$

$$w_{2,19}(t, x) = -s_1 \sqrt{-\frac{k}{m}} \left(\coth(2\sqrt{-km}\varphi) + (\operatorname{csch}(2\sqrt{-km}\varphi)) \right), \quad (3.58)$$

$$w_{2,20}(t, x) = -\frac{1}{2} s_1 \sqrt{-\frac{k}{m}} \left(\tanh\left(\frac{1}{2}\sqrt{km}\varphi\right) + \coth\left(\frac{1}{2}\sqrt{-km}\varphi\right) \right). \quad (3.59)$$

Family 2.5. For $m = k$ and $l = 0$:

$$w_{2,21}(t, x) = s_1 \tan(m\varphi), \quad (3.60)$$

$$w_{2,22}(t, x) = -s_1 \cot(m\varphi), \quad (3.61)$$

$$w_{2,23}(t, x) = s_1 (\tan(2m\varphi) + \sec(2m\varphi)), \quad (3.62)$$

$$w_{2,24}(t, x) = s_1 (-\cot(2m\varphi) + \csc(2m\varphi)), \quad (3.63)$$

$$w_{2,25}(t, x) = \frac{1}{2} s_1 \tan\left(\frac{1}{2}m\varphi\right). \quad (3.64)$$

Family 2.6. For $m = -k$ and $l = 0$:

$$w_{2,26}(t, x) = -s_1 \tanh(k\varphi), \quad (3.65)$$

$$w_{2,27}(t, x) = -s_1 \coth(k\varphi), \quad (3.66)$$

$$w_{2,28}(t, x) = s_1 (-\tanh(2k\varphi) + \operatorname{isech}(2k\varphi)), \quad (3.67)$$

$$w_{2,29}(t, x) = s_1 (-\coth(2k\varphi) + \operatorname{csch}(2k\varphi)), \quad (3.68)$$

$$w_{2,30}(t, x) = s_1 \left(-\frac{1}{2} \tanh\left(\frac{1}{2}k\varphi\right) - \frac{1}{2} \coth\left(\frac{1}{2}k\varphi\right) \right). \quad (3.69)$$

Family 2.7. For $\Omega = 0$:

$$w_{2,31}(t, x) = \frac{s_{-1}l}{2m} - 2 \frac{s_1 k (l\varphi + 2)}{l^2 \varphi}. \quad (3.70)$$

Family 2.8. For $l = k = 0$:

$$w_{2,32}(t, x) = -\frac{s_1}{m\varphi}. \quad (3.71)$$

Family 2.9. For $l \neq 0, m \neq 0$ and $k = 0$:

$$w_{2,33}(t, x) = \frac{s_{-1}l}{2m} - \frac{s_1 l}{m (\cosh(l\varphi) - \sinh(l\varphi) + 1)}, \quad (3.72)$$

$$w_{2,34}(t, x) = \frac{s_{-1}l}{2m} - \frac{s_1 l}{m}. \quad (3.73)$$

Family 2.10. For $l = \kappa, m = n\kappa$ (with $n \neq 0$), and $k = 0$:

$$w_{2,35}(t, x) = \frac{s_{-1}\kappa}{2n\kappa} + \frac{s_1 e^{\kappa\varphi}}{1 - ne^{\Omega\varphi}}. \quad (3.74)$$

In the above solutions, $\varphi = x + \omega t$.

By taking into account Case 3 and using Eqs (3.1) and (3.2) with the corresponding solution of (2.4), we produce the following plethora of soliton solutions for PFE stated in (1.3):

Family 3.1. For $\Omega < 0$ and $m \neq 0$:

$$w_{3,1}(t, x) = s_0 + s_{-1} \left(-\frac{l}{2m} + \frac{\sqrt{-\Omega} \tan\left(\frac{1}{2} \sqrt{-\Omega}\varphi\right)}{2m} \right)^{-1} + s_1 \left(-\frac{l}{2m} + \frac{\sqrt{-\Omega} \tan\left(\frac{1}{2} \sqrt{-\Omega}\varphi\right)}{2m} \right), \quad (3.75)$$

$$w_{3,2}(t, x) = s_0 + s_{-1} \left(-\frac{l}{2m} - \frac{\sqrt{-\Omega} \cot\left(\frac{1}{2} \sqrt{-\Omega}\varphi\right)}{2m} \right)^{-1} + s_1 \left(-\frac{l}{2m} - \frac{\sqrt{-\Omega} \cot\left(\frac{1}{2} \sqrt{-\Omega}\varphi\right)}{2m} \right), \quad (3.76)$$

$$w_{3,3}(t, x) = s_0 + s_{-1} \left(-\frac{l}{2m} + \frac{\sqrt{-\Omega} (\tan(\sqrt{-\Omega}\varphi) + \sec(\sqrt{-\Omega}\varphi))}{2m} \right)^{-1} + s_1 \left(-\frac{l}{2m} + \frac{\sqrt{-\Omega} (\tan(\sqrt{-\Omega}\varphi) + \sec(\sqrt{-\Omega}\varphi))}{2m} \right), \quad (3.77)$$

$$w_{3,4}(t, x) = s_0 + s_{-1} \left(-\frac{1}{2} \frac{l}{m} - \frac{1}{2} \frac{\sqrt{-\Omega} (\cot(\sqrt{-\Omega}\varphi) + \csc(\sqrt{-\Omega}\varphi))}{m} \right)^{-1} + s_1 \left(-\frac{1}{2} \frac{l}{m} - \frac{1}{2} \frac{\sqrt{-\Omega} (\cot(\sqrt{-\Omega}\varphi) + \csc(\sqrt{-\Omega}\varphi))}{m} \right), \quad (3.78)$$

$$w_{3,5}(t, x) = s_0 + s_{-1} \left(-\frac{l}{2m} + \frac{\sqrt{-\Omega} \left(\tan\left(\frac{1}{4} \sqrt{-\Omega} \varphi\right) - \cot\left(\frac{1}{4} \sqrt{-\Omega} \varphi\right) \right)}{4m} \right)^{-1} + s_1 \left(-\frac{l}{2m} + \frac{\sqrt{-\Omega} \left(\tan\left(\frac{1}{4} \sqrt{-\Omega} \varphi\right) - \cot\left(\frac{1}{4} \sqrt{-\Omega} \varphi\right) \right)}{4m} \right). \quad (3.79)$$

Family 3.2. For $\Omega > 0$ and $m \neq 0$:

$$w_{3,6}(t, x) = s_0 + s_{-1} \left(-\frac{l}{2m} - \frac{\sqrt{\Omega} \tanh(\sqrt{\Omega} \varphi)}{2m} \right)^{-1} + s_1 \left(-\frac{l}{2m} - \frac{1}{2} \frac{\sqrt{\Omega} \tanh(\sqrt{\Omega} \varphi)}{m} \right), \quad (3.80)$$

$$w_{3,7}(t, x) = s_0 + s_{-1} \left(-\frac{l}{2m} - \frac{\sqrt{\Omega} \coth\left(\frac{1}{2} \sqrt{\Omega} \varphi\right)}{2m} \right)^{-1} + s_1 \left(-\frac{l}{2m} - \frac{\sqrt{\Omega} \coth\left(\frac{1}{2} \sqrt{\Omega} \varphi\right)}{2m} \right), \quad (3.81)$$

$$w_{3,8}(t, x) = s_0 + s_{-1} \left(-\frac{l}{2m} - \frac{\sqrt{\Omega} \left(\tanh(\sqrt{\Omega} \varphi) + i \operatorname{sech}(\sqrt{\Omega} \varphi) \right)}{2m} \right)^{-1} + s_1 \left(-\frac{l}{2m} - \frac{\sqrt{\Omega} \left(\tanh(\sqrt{\Omega} \varphi) + i \operatorname{sech}(\sqrt{\Omega} \varphi) \right)}{2m} \right), \quad (3.82)$$

$$w_{3,9}(t, x) = s_0 + s_{-1} \left(-\frac{l}{2m} - \frac{\sqrt{\Omega} \left(\coth(\sqrt{\Omega} \varphi) + \operatorname{csch}(\sqrt{\Omega} \varphi) \right)}{2m} \right)^{-1} + s_1 \left(-\frac{l}{2m} - \frac{\sqrt{\Omega} \left(\coth(\sqrt{\Omega} \varphi) + \operatorname{csch}(\sqrt{\Omega} \varphi) \right)}{2m} \right), \quad (3.83)$$

$$w_{3,10}(t, x) = s_0 + s_{-1} \left(-\frac{l}{2m} - \frac{\sqrt{\Omega} \left(\tanh\left(\frac{1}{4} \sqrt{\Omega} \varphi\right) - \coth\left(\frac{1}{4} \sqrt{\Omega} \varphi\right) \right)}{4m} \right)^{-1} + s_1 \left(-\frac{l}{2m} - \frac{\sqrt{\Omega} \left(\tanh\left(\frac{1}{4} \sqrt{\Omega} \varphi\right) - \coth\left(\frac{1}{4} \sqrt{\Omega} \varphi\right) \right)}{4m} \right). \quad (3.84)$$

Family 3.3. For $km > 0$ and $l = 0$:

$$w_{3,11}(t, x) = s_0 + s_{-1} \sqrt{\frac{m}{k}} \left(\tan(\sqrt{mk} \varphi) \right)^{-1} + s_1 \sqrt{\frac{k}{m}} \tan(\sqrt{mk} \varphi), \quad (3.85)$$

$$w_{3,12}(t, x) = s_0 - s_{-1} \sqrt{\frac{m}{k}} \left(\cot(\sqrt{mk} \varphi) \right)^{-1} - s_1 \sqrt{\frac{k}{m}} \cot(\sqrt{mk} \varphi), \quad (3.86)$$

$$w_{3,13}(t, x) = s_0 + s_{-1} \sqrt{\frac{m}{k}} \left(\tan(2 \sqrt{mk} \varphi) + \sec(2 \sqrt{mk} \varphi) \right)^{-1} + s_1 \sqrt{\frac{k}{m}} \left(\tan(2 \sqrt{mk} \varphi) + \sec(2 \sqrt{mk} \varphi) \right), \quad (3.87)$$

$$w_{3,14}(t, x) = s_0 - s_{-1} \sqrt{\frac{m}{k}} \left(\cot(2\sqrt{mk}\varphi) + \csc(2\sqrt{mk}\varphi) \right)^{-1} - s_1 \sqrt{\frac{k}{m}} \left(\cot(2\sqrt{mk}\varphi) + \csc(2\sqrt{mk}\varphi) \right), \quad (3.88)$$

$$w_{3,15}(t, x) = s_0 + 2s_{-1} \sqrt{\frac{m}{k}} \left(\tan\left(\frac{1}{2}\sqrt{mk}\varphi\right) - \cot\left(\frac{1}{2}\sqrt{mk}\varphi\right) \right)^{-1} + \frac{1}{2}s_1 \sqrt{\frac{k}{m}} \left(\tan\left(\frac{1}{2}\sqrt{mk}\varphi\right) - \cot\left(\frac{1}{2}\sqrt{mk}\varphi\right) \right). \quad (3.89)$$

Family 3.4. For $km < 0$ and $l = 0$:

$$w_{3,16}(t, x) = s_0 - s_{-1} \sqrt{-\frac{m}{k}} \left(\tanh(\sqrt{-mk}\varphi) \right)^{-1} - s_1 \sqrt{-\frac{k}{m}} \tanh(\sqrt{-mk}\varphi), \quad (3.90)$$

$$w_{3,17}(t, x) = s_0 - s_{-1} \sqrt{-\frac{m}{k}} \left(\coth(\sqrt{-mk}\varphi) \right)^{-1} - s_1 \sqrt{-\frac{k}{m}} \coth(\sqrt{-mk}\varphi), \quad (3.91)$$

$$w_{3,18}(t, x) = s_0 - s_{-1} \sqrt{-\frac{m}{k}} \left(\tanh(2\sqrt{-km}\varphi) + (\operatorname{isech}(2\sqrt{-km}\varphi)) \right)^{-1} - s_1 \sqrt{-\frac{k}{m}} \left(\tanh(2\sqrt{-km}\varphi) + (\operatorname{isech}(2\sqrt{-km}\varphi)) \right), \quad (3.92)$$

$$w_{3,19}(t, x) = s_0 - s_{-1} \sqrt{-\frac{m}{k}} \left(\coth(2\sqrt{-km}\varphi) + (\operatorname{csch}(2\sqrt{-km}\varphi)) \right)^{-1} - s_1 \sqrt{-\frac{k}{m}} \left(\coth(2\sqrt{-km}\varphi) + (\operatorname{csch}(2\sqrt{-km}\varphi)) \right), \quad (3.93)$$

$$w_{3,20}(t, x) = s_0 - 2s_{-1} \sqrt{-\frac{m}{k}} \left(\tanh\left(\frac{1}{2}\sqrt{km}\varphi\right) + \coth\left(\frac{1}{2}\sqrt{-km}\varphi\right) \right)^{-1} - \frac{1}{2}s_1 \sqrt{-\frac{k}{m}} \left(\tanh\left(\frac{1}{2}\sqrt{km}\varphi\right) + \coth\left(\frac{1}{2}\sqrt{-km}\varphi\right) \right). \quad (3.94)$$

Family 3.5. For $m = k$ and $l = 0$:

$$w_{3,21}(t, x) = s_0 + \frac{s_{-1}}{\tan(m\varphi)} + s_1 \tan(m\varphi). \quad (3.95)$$

$$w_{3,22}(t, x) = s_0 - \frac{s_{-1}}{\cot(m\varphi)} - s_1 \cot(m\varphi), \quad (3.96)$$

$$w_{3,23}(t, x) = s_0 + \frac{s_{-1}}{\tan(2m\varphi) + \sec(2m\varphi)} + s_1 (\tan(2m\varphi) + \sec(2m\varphi)), \quad (3.97)$$

$$w_{3,24}(t, x) = s_0 + \frac{s_{-1}}{-\cot(2m\varphi) + \csc(2m\varphi)} + s_1 (-\cot(2m\varphi) + \csc(2m\varphi)), \quad (3.98)$$

$$w_{3,25}(t, x) = s_0 + \frac{s_{-1}}{\frac{1}{2}\tan\left(\frac{1}{2}m\varphi\right) - \frac{1}{2}\cot\left(\frac{1}{2}m\varphi\right)} + s_1 \left(\frac{1}{2}\tan\left(\frac{1}{2}m\varphi\right) - \frac{1}{2}\cot\left(\frac{1}{2}m\varphi\right) \right). \quad (3.99)$$

Family 3.6. For $m = -k$ and $l = 0$:

$$w_{3,26}(t, x) = s_0 - \frac{s_{-1}}{\tanh(k\varphi)} - s_1 \tanh(k\varphi), \quad (3.100)$$

$$w_{3,27}(t, x) = s_0 - \frac{s_{-1}}{\coth(k\varphi)} - s_1 \coth(k\varphi), \quad (3.101)$$

$$w_{3,28}(t, x) = s_0 + \frac{s_{-1}}{-\tanh(2k\varphi) + i \operatorname{sech}(2k\varphi)} + s_1 (-\tanh(2k\varphi) + i \operatorname{sech}(2k\varphi)), \quad (3.102)$$

$$w_{3,29}(t, x) = s_0 + \frac{s_{-1}}{-\coth(2k\varphi) + \operatorname{csch}(2k\varphi)} + s_1 (-\coth(2k\varphi) + \operatorname{csch}(2k\varphi)), \quad (3.103)$$

$$w_{3,30}(t, x) = s_0 + \frac{s_{-1}}{-\frac{1}{2} \tanh\left(\frac{1}{2}k\varphi\right) - \frac{1}{2} \coth\left(\frac{1}{2}k\varphi\right)} + s_1 \left(-\frac{1}{2} \tanh\left(\frac{1}{2}k\varphi\right) - \frac{1}{2} \coth\left(\frac{1}{2}k\varphi\right) \right). \quad (3.104)$$

Family 3.7. For $\Omega = 0$:

$$w_{3,31}(t, x) = s_0 - \frac{1}{2} \frac{s_{-1} l^2 \varphi}{k(k\varphi + 2)} - 2 \frac{s_1 k(k\varphi + 2)}{l^2 \varphi}. \quad (3.105)$$

Family 3.8. For $m = 0$, $l = \kappa$ and $k = n\kappa$ (with $n \neq 0$).

$$w_{3,32}(t, x) = s_0 + \frac{s_{-1}}{e^{\kappa\Omega} - n} + s_1 (e^{\kappa\Omega} - n). \quad (3.106)$$

Family 3.9. For $l = m = 0$:

$$w_{3,33}(t, x) = s_0 + \frac{s_{-1}}{k\eta} + s_1 k\eta. \quad (3.107)$$

Family 3.10. For $l = k = 0$:

$$w_{3,34}(t, x) = s_0 - s_{-1} m\varphi - \frac{s_1}{m\varphi}. \quad (3.108)$$

Family 3.11. For $l \neq 0$, $m \neq 0$ and $k = 0$:

$$w_{3,35}(t, x) = s_0 - \frac{s_{-1} m (\cosh(l\varphi) - \sinh(l\varphi) + 1)}{l} - \frac{s_1 l}{m (\cosh(l\varphi) - \sinh(l\varphi) + 1)}, \quad (3.109)$$

$$w_{3,36}(t, x) = s_0 - \frac{s_{-1} m}{l} - \frac{s_1 l}{m}. \quad (3.110)$$

Family 3.12. For $l = \kappa$, $m = n\kappa$ (with $n \neq 0$), and $k = 0$:

$$w_{3,37}(t, x) = s_0 + \frac{s_{-1} (1 - ne^{\kappa\varphi})}{e^{\kappa\varphi}} + \frac{s_1 e^{\kappa\varphi}}{1 - ne^{\kappa\varphi}}. \quad (3.111)$$

In the above solutions, $\varphi = x \pm t$.

4. Discussion and graphs

We provide illustrations of the various wave structures present in the system under investigation in this section. We extracted and prominently displayed wave patterns such kink, shock, bright-dark, hump, lump-type, dromion, and periodic soliton in 3D, 2D, and contour forms using EDAM. To the very best of our knowledge, the utilization of EDAM to the PFE has not previously been documented in scientific literature, which makes the study's findings unique. These findings are critical to comprehending how linked physical phenomena behave. The goal of the developed soliton solutions is to greatly advance our understanding of nonlinear physics, namely particle, condensed matter, and cosmological physics. Additionally, it has been demonstrated that the approach taken in this work is highly successful, reliable, and applicable to nonlinear issues across a range of natural science fields. Figure 1, the 3D, contour and 2D depictions of the dromion soliton solution $w_{1,2}$ articulated in (3.8) are visualized for $k := 3; l := 4; m := 2; s_{-1} := 4; \omega := 7$. Plotting of the 2D graph is done concurrently for $t = 0$ and the same values of the related parameters. Figure 2, the 3D, contour and 2D depictions of the periodic hump soliton solution $w_{1,10}$ articulated in (3.16) are visualized for $k := 2; l := 5; m := 2; s_{-1} := 4; \omega := 5$. Plotting of the 2D graph is done concurrently for $t = 0$ and the same values of the related parameters. Figure 3, the 3D, contour and 2D depictions of the shock soliton solution $w_{1,33}$ articulated in (3.39) are visualized for $k := 3; l := 0; m := 0; s_{-1} := 4; \omega := 5$. Plotting of the 2D graph is done concurrently for $t = 0$ and the same values of the related parameters. Figure 4, the 3D, contour and 2D depictions of the kink soliton solution $w_{2,6}$ articulated in (3.45) are visualized for $k := 2; l := 6; m := 2; s_1 := 4; s_{-1} := 8; \omega := 4$. Plotting of the 2D graph is done concurrently for $t = 0$ and the same values of the related parameters. Figure 5, the 3D, contour and 2D depictions of the lump-type kink soliton solution $w_{2,12}$ articulated in (3.51) are visualized for $k := 2; l := 1; m := 2; s_1 := 4; s_{-1} := 8; s_0 := 5; \omega := 4$. Plotting of the 2D graph is done concurrently for $t = 1$ and the same values of the related parameters.

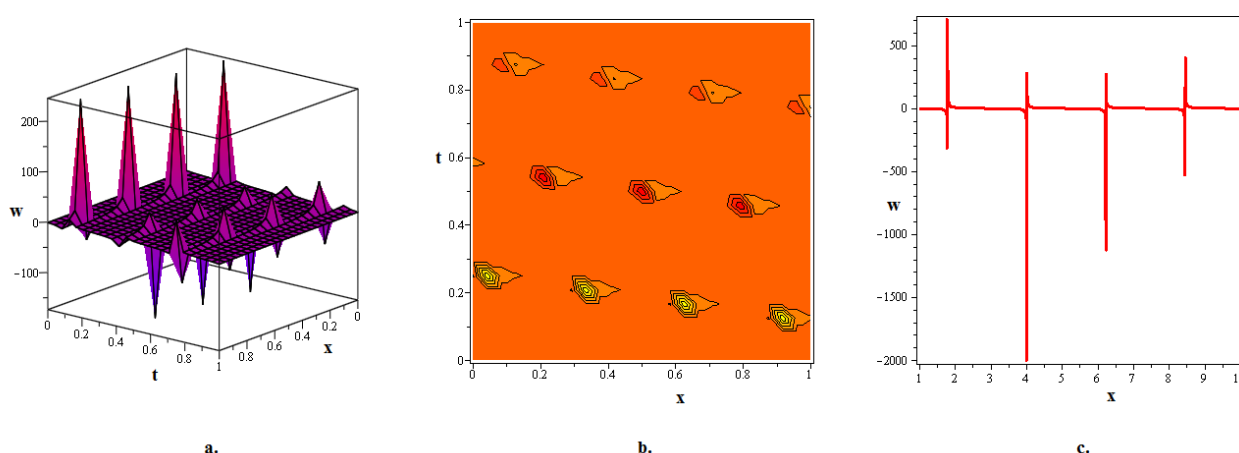


Figure 1. The 3D, contour and 2D depictions of the dromion soliton solution $w_{1,2}$ articulated in (3.8) are visualized for $k := 3; l := 4; m := 2; s_{-1} := 4; \omega := 7$. Plotting of the 2D graph is done concurrently for $t = 0$ and the same values of the related parameters.

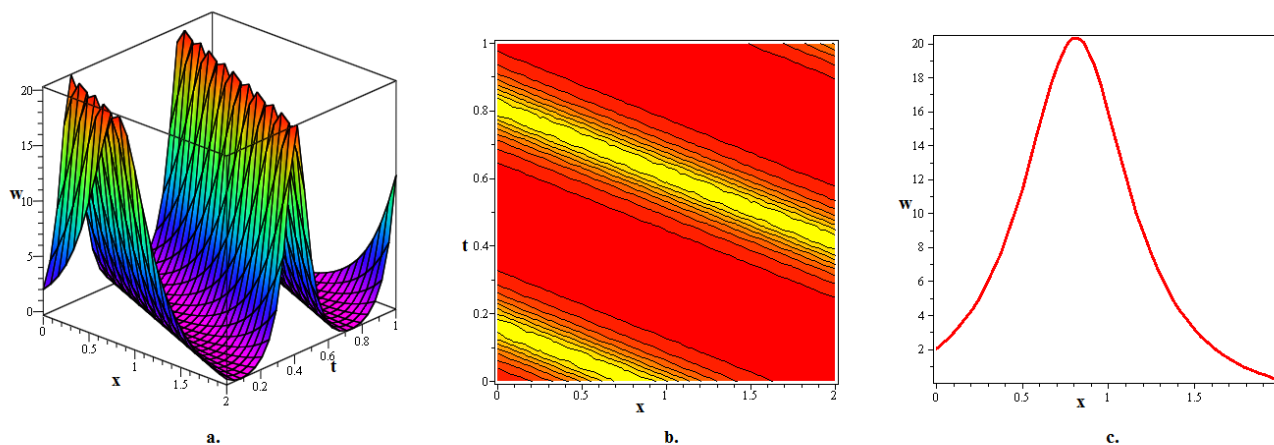


Figure 2. The 3D, contour and 2D depictions of the periodic hump soliton solution $w_{1,10}$ articulated in (3.16) are visualized for $k := 2; l := 5; m := 2; s_{-1} := 4; \omega := 5$. Plotting of the 2D graph is done concurrently for $t = 0$ and the same values of the related parameters.

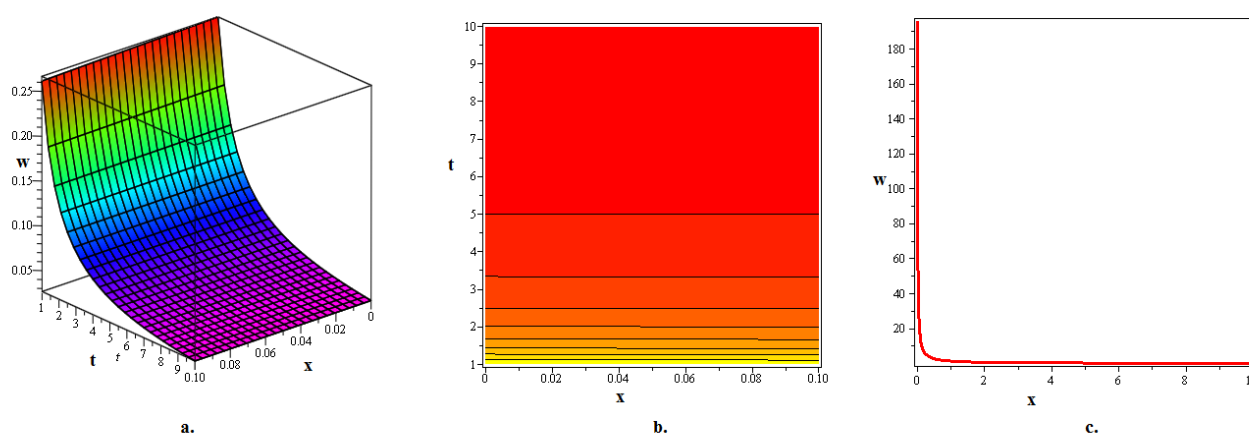


Figure 3. The 3D, contour and 2D depictions of the shock soliton solution $w_{1,33}$ articulated in (3.39) are visualized for $k := 3; l := 0; m := 0; s_{-1} := 4; \omega := 5$. Plotting of the 2D graph is done concurrently for $t = 0$ and the same values of the related parameters.

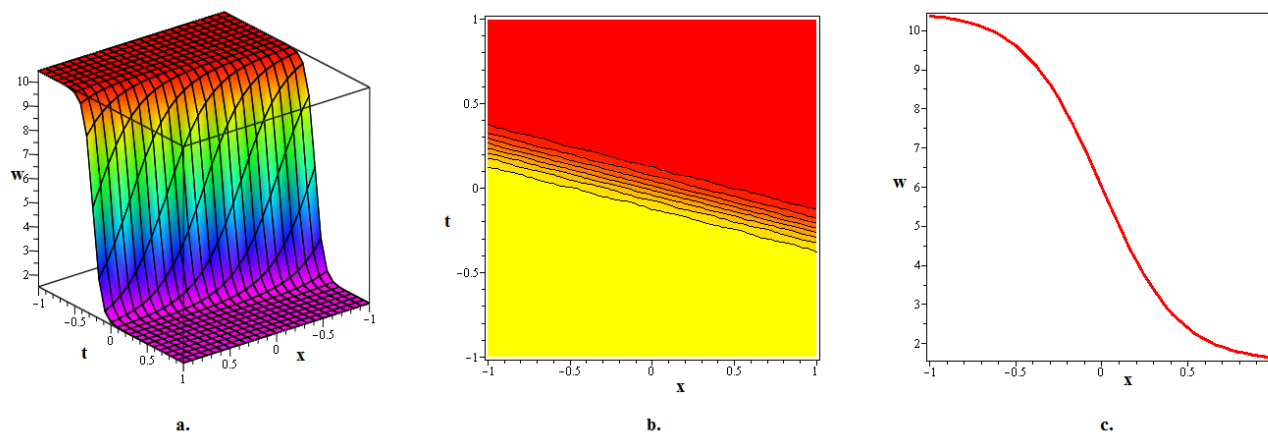


Figure 4. The 3D, contour and 2D depictions of the kink soliton solution $w_{2,6}$ articulated in (3.45) are visualized for $k := 2; l := 6; m := 2; s_1 := 4; s_{-1} := 8; \omega := 4$. Plotting of the 2D graph is done concurrently for $t = 0$ and the same values of the related parameters.

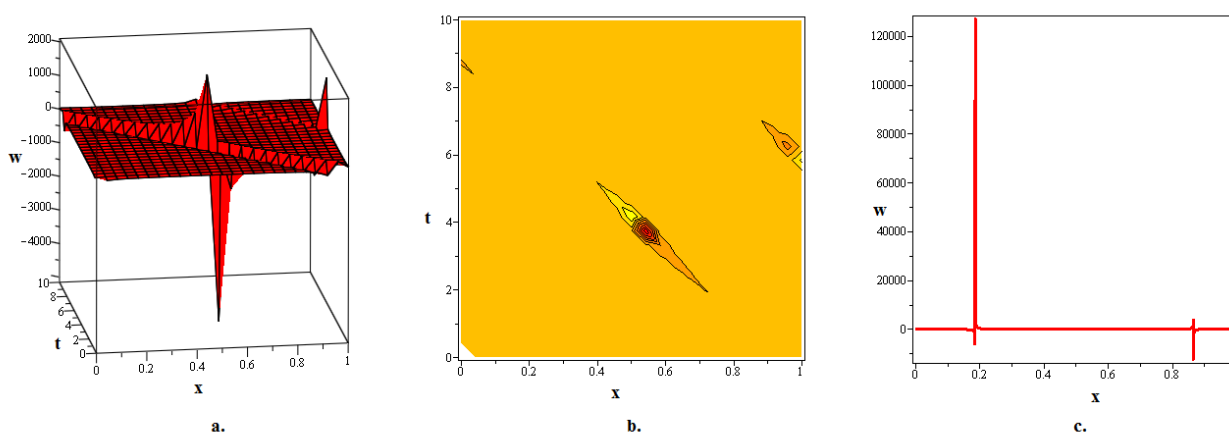


Figure 5. The 3D, contour and 2D depictions of the lump-type kink soliton solution $w_{2,12}$ articulated in (3.51) are visualized for $k := 2; l := 1; m := 2; s_1 := 4; s_{-1} := 8; s_0 := 5; \omega := 4$. Plotting of the 2D graph is done concurrently for $t = 1$ and the same values of the related parameters.

Within the context of the PFE, the different kinds of solitons offer discrete wavelike solutions with distinct properties and applications in subatomic and condensed-state physics, among other fields. Because of their flexible, step-like transit between states, kink solitons can be used to simulate phase transitions or domain borders. Because of their abrupt changes, shock solitons can be compared to shock waves in systems. Bright-dark type solitons are made up of localized zones of low intensity (dark) and extreme intensity (bright), which are comparable to the interactions between particles or stimulation in a material. Compact solitons, like a lump, are utilized to simulate phenomena such

as isolated waveform impulses in systems that are magnetized. They show localized waves with a raised level (hump) or a localized wave that is falling (lump). Dromion solitaires are shape-preserving, localized, complex waves connected to particle-like excitation. The recurrent, waveform-like structures shown by periodic solitons can be exploited to mimic wave patterns and oscillations in a range of media. All in all, these solitons exhibit complex behaviors in nonlinear frameworks and are helpful in understanding phase transitions, wave propagation, and particle-like excitations in a range of fields. The soliton solutions in terms of trigonometric functions nearly resemble periodic, dromion, and lump-type soliton; those in terms of hyperbolic functions nearly resemble kink solitons; and those in terms of rational or exponential functions nearly resemble shock solitons, according to our overall analyses of the soliton solutions. Figure 6, the 3D, contour and 2D depictions of the shock soliton solution $w_{2,32}$ articulated in (3.71) are visualized for $k := 0; l := 0; m := 2; s_1 := 4; s_{-1} := 8; \omega := 4$. Plotting of the 2D graph is done concurrently for $t = 1$ and the same values of the related parameters. Figure 7, the 3D, contour and 2D depictions of the dromion soliton solution $w_{3,2}$ articulated in (3.76) are visualized for $k := 2; l := 1; m := 2; s_1 := 4; s_{-1} := 8; s_0 := 5; \omega := 1$. Plotting of the 2D graph is done concurrently for $t = 10$ and the same values of the related parameters. Figure 8, the 3D, contour and 2D depictions of the 2-kink soliton solution $w_{3,6}$ articulated in (3.80) are visualized for $k := 36; l := 13; m := 1; s_1 := 4; s_{-1} := 8; s_0 := 5; \omega := 1$. Plotting of the 2D graph is done concurrently for $t = 5$ and the same values of the related parameters. Figure 9, the 3D, contour and 2D depictions of the bright-dark soliton solution (also called breather soliton) $w_{3,21}$ articulated in (3.95) are visualized for $k := 2; l := 0; m := 2; s_1 := 4; s_{-1} := 8; s_0 := 5; \omega := -1$. Plotting of the 2D graph is done concurrently for $t = 0$ and the same values of the related parameters. Figure 10, the 3D, contour and 2D depictions of the kink soliton solution $w_{3,26}$ articulated in (3.100) are visualized for $k := -2; l := 0; m := 2; s_1 := 4; s_{-1} := 10; s_0 := 5; \omega := -1$. Plotting of the 2D graph is done concurrently for $t = 0.5$ and the same values of the related parameters.

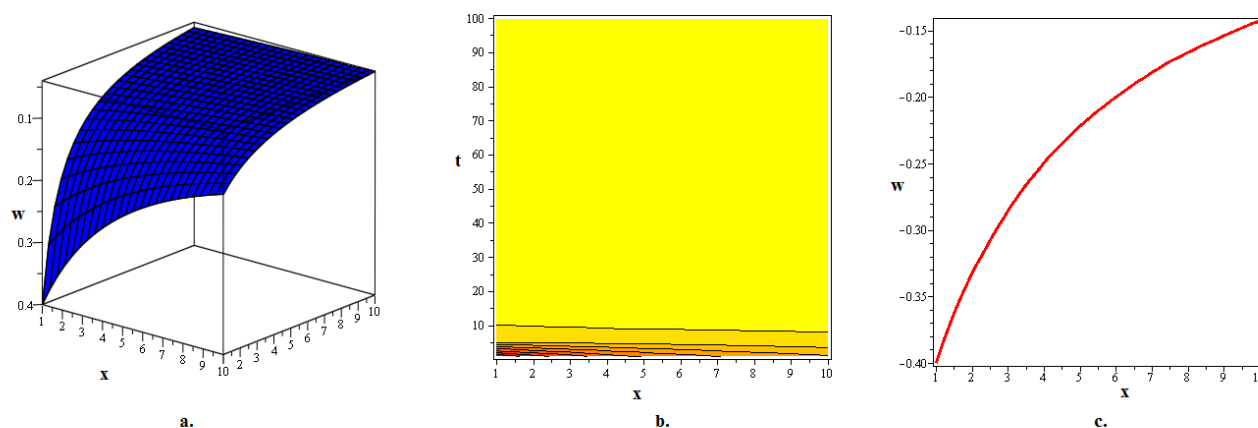


Figure 6. The 3D, contour and 2D depictions of the shock soliton solution $w_{2,32}$ articulated in (3.71) are visualized for $k := 0; l := 0; m := 2; s_1 := 4; s_{-1} := 8; \omega := 4$. Plotting of the 2D graph is done concurrently for $t = 1$ and the same values of the related parameters.

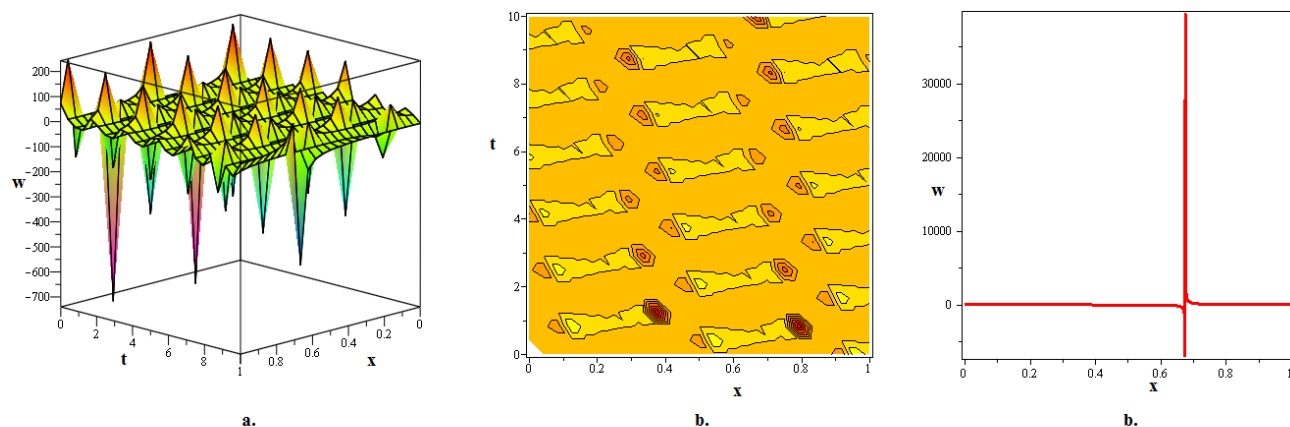


Figure 7. The 3D, contour and 2D depictions of the dromion soliton solution $w_{3,2}$ articulated in (3.76) are visualized for $k := 2; l := 1; m := 2; s_1 := 4; s_{-1} := 8; s_0 := 5; \omega := 1$. Plotting of the 2D graph is done concurrently for $t = 10$ and the same values of the related parameters.

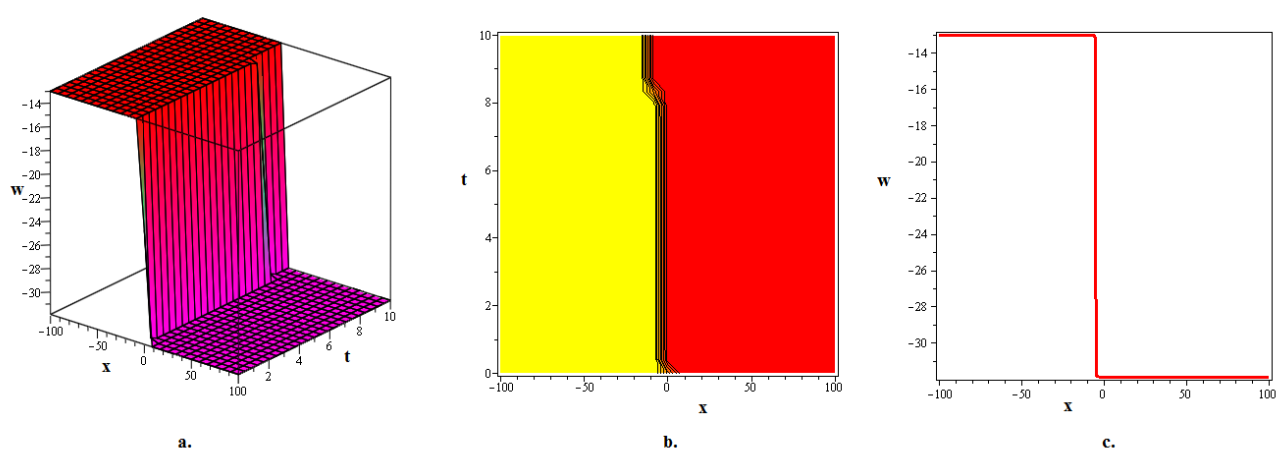


Figure 8. The 3D, contour and 2D depictions of the 2-kink soliton solution $w_{3,6}$ articulated in (3.80) are visualized for $k := 36; l := 13; m := 1; s_1 := 4; s_{-1} := 8; s_0 := 5; \omega := 1$. Plotting of the 2D graph is done concurrently for $t = 5$ and the same values of the related parameters.

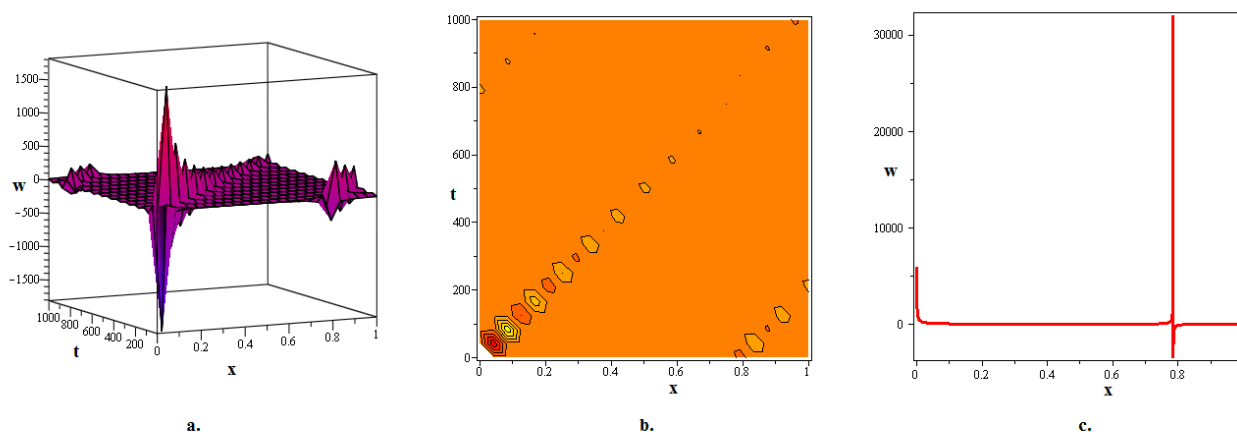


Figure 9. The 3D, contour and 2D depictions of the bright-dark soliton solution (also called breather soliton) $w_{3,21}$ articulated in (3.95) are visualized for $k := 2; l := 0; m := 2; s_1 := 4; s_{-1} := 8; s_0 := 5; \omega := -1$. Plotting of the 2D graph is done concurrently for $t = 0$ and the same values of the related parameters.

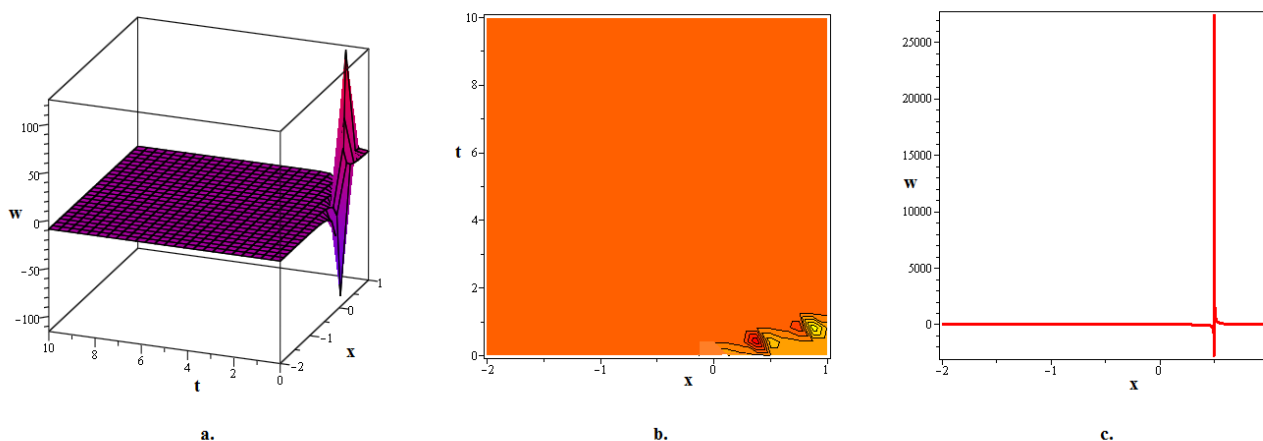


Figure 10. The 3D, contour and 2D depictions of the kink soliton solution $w_{3,26}$ articulated in (3.100) are visualized for $k := -2; l := 0; m := 2; s_1 := 4; s_{-1} := 10; s_0 := 5; \omega := -1$. Plotting of the 2D graph is done concurrently for $t = 0.5$ and the same values of the related parameters.

5. Conclusions

This investigation addressed PFE with the enhanced EDAM. For the given system of NODE that the challenge produced, the EDAM was able to discover a series form solution. In order to achieve propagating soliton solutions which are crucial to the problem's physical interpretation this solution was subsequently molded into a system of nonlinear algebraic equations. Many traveling waves,

including kink, shock, bright-dark, hump, lump-type, and dromion, were shown to occur in soliton solutions through the display of multiple 3D, 2D, and contour graphs. In addition to highlighting the implications for a number of real-world applications in the related domains of nonlinear physics, including subatomic and condensed-state physics, the essay shows how the EDAM can be used to construct families of soliton solutions for challenging issues. Even while the EDAM has greatly improved our knowledge of soliton dynamics and how they relate to the models we are studying, it is crucial to recognize the drawbacks of this approach, especially in cases where the nonlinear term and greatest derivative are not uniformly balanced. The study emphasises the necessity for more research on soliton patterns and nonlinear behavior in spite of this flaw. The study's recommendations for the future are to investigate soliton events in stochastic nonlinear models and adapt the approach to nonlinear models with variable coefficients.

Author contributions

Mohammed Aldandani, Abdulhadi A. Altherwi and Mastoor M. Abushaega: Conceptualization, Methodology, Validation, Writing-original draft, Writing-review & editing. All authors contributed equally and approved the final version of the current manuscript.

Use of AI tools declaration

The authors declare they have not used Artificial Intelligence (AI) tools in the creation of this article.

Acknowledgments

The authors gratefully acknowledge the funding of the Deanship of Graduate Studies and Scientific Research, Jazan University, Saudi Arabia, through Project Number: GSSRD-24.

Conflict of interest

The authors declare no conflict of interest.

References

1. W. Gao, H. Rezazadeh, Z. Pinar, H. Baskonus, S. Sarwar, G. Yel, Novel explicit solutions for the nonlinear Zoomeron equation by using newly extended direct algebraic technique, *Opt. Quant. Electron.*, **52** (2020), 52. <http://dx.doi.org/10.1007/s11082-019-2162-8>
2. M. Khater, Solitary wave solutions for the generalized Zakharov-Kuznetsov-Benjamin-Bona-Mahony nonlinear evolution equation, *Global J. Sci. Front. Res. Phys. Space Sci.*, **16** (2016), 37–41.
3. H. Bulut, T. Sulaiman, H. Baskonus, H. Rezazadeh, M. Eslami, M. Mirzazadeh, Optical solitons and other solutions to the conformable space time fractional Fokas Lenells equation, *Optik*, **172** (2018), 20–27. <http://dx.doi.org/10.1016/j.ijleo.2018.06.108>

4. S. Vlase, M. Marin, A. Öchsner, M. Scutaru, Motion equation for a flexible one-dimensional element used in the dynamical analysis of a multibody system, *Continuum Mech. Thermodyn.*, **31** (2019), 715–724. <http://dx.doi.org/10.1007/s00161-018-0722-y>
5. M. Khater, A. Seadawy, D. Lu, Bifurcations of solitary wave solutions for (two and three)-dimensional nonlinear partial differential equation in quantum and magnetized plasma by using two different methods, *Results Phys.*, **9** (2018), 142–150. <http://dx.doi.org/10.1016/j.rinp.2018.02.010>
6. V. Senthil Kumar, H. Rezazadeh, M. Eslami, F. Izadi, M. Osman, Jacobi elliptic function expansion method for solving KdV equation with conformable derivative and dual-power law nonlinearity, *Int. J. Appl. Comput. Math.*, **5** (2019), 127. <http://dx.doi.org/10.1007/s40819-019-0710-3>
7. M. Khater, A. Seadawy, D. Lu, Dispersive solitary wave solutions of new coupled Konno-Oono, Higgs field and Maccari equations and their applications, *J. King Saud Univ. Sci.*, **30** (2018), 417–423. <http://dx.doi.org/10.1016/j.jksus.2017.11.003>
8. M. Ghasemi, High order approximations using spline-based differential quadrature method: implementation to the multi-dimensional PDEs, *Appl. Math. Model.*, **46** (2017), 63–80. <http://dx.doi.org/10.1016/j.apm.2017.01.052>
9. S. Noor, W. Albalawi, R. Shah, M. Mossa Al-Sawalha, S. Ismaeel, S. El-Tantawy, On the approximations to fractional nonlinear damped Burger's-type equations that arise in fluids and plasmas using Aboodh residual power series and Aboodh transform iteration methods, *Front. Phys.*, **12** (2024), 1374481. <http://dx.doi.org/10.3389/fphy.2024.1374481>
10. N. Perrone, R. Kao, A general finite difference method for arbitrary meshes, *Comput. Struct.*, **5** (1975), 45–57. [http://dx.doi.org/10.1016/0045-7949\(75\)90018-8](http://dx.doi.org/10.1016/0045-7949(75)90018-8)
11. M. Abdou, A. Soliman, New applications of variational iteration method, *Physica D*, **211** (2005), 1–8. <http://dx.doi.org/10.1016/j.physd.2005.08.002>
12. M. Hammad, R. Shah, B. Alotaibi, M. Alotiby, C. Tiofack, A. Alrowaily, et al., On the modified versions of $\frac{G'}{G}$ -expansion technique for analyzing the fractional coupled Higgs system, *AIP Adv.*, **13** (2023), 105131. <http://dx.doi.org/10.1063/5.0167916>
13. E. Yusufoglu, A. Bekir, Solitons and periodic solutions of coupled nonlinear evolution equations by using the sine cosine method, *Int. J. Comput. Math.*, **83** (2006), 915–924. <http://dx.doi.org/10.1080/00207160601138756>
14. Y. Chen, B. Li, H. Zhang, Generalized Riccati equation expansion method and its application to the Bogoyavlenskii's generalized breaking soliton equation, *Chinese Phys.*, **12** (2003), 940. <http://dx.doi.org/10.1088/1009-1963/12/9/303>
15. H. Liu, T. Zhang, A note on the improved $\tan(\phi(\xi)/2)$ -expansion method, *Optik*, **131** (2017), 273–278. <http://dx.doi.org/10.1016/j.ijleo.2016.11.029>
16. M. Guo, H. Dong, J. Liu, H. Yang, The time-fractional mZK equation for gravity solitary waves and solutions using sech-tanh and radial basic function method, *Nonlinear Anal.-Model.*, **24** (2018), 1–19. <http://dx.doi.org/10.15388/NA.2019.1.1>
17. M. Kaplan, A. Bekir, A. Akbulut, E. Aksoy, The modified simple equation method for nonlinear fractional differential equations, *Rom. J. Phys.*, **60** (2015), 1374–1383.

18. K. L. Wang, K. J. Wang, C. He, Physical insight of local fractional calculus and its application to fractional Kdv-Burgers-Kuramoto equation, *Fractals*, **27** (2019), 1950122. <http://dx.doi.org/10.1142/S0218348X19501226>
19. K. L. Wang, K. J. Wang, A modification of the reduced differential transform method for fractional calculus, *Therm. Sci.*, **22** (2018), 1871–1875. <http://dx.doi.org/10.2298/TSCI1804871W>
20. K. J. Wang, On a high-pass filter described by local fractional derivative, *Fractals*, **28** (2020), 2050031. <http://dx.doi.org/10.1142/S0218348X20500310>
21. R. Ali, Z. Zhang, H. Ahmad, Exploring soliton solutions in nonlinear spatiotemporal fractional quantum mechanics equations: an analytical study, *Opt. Quant. Electron.*, **56** (2024), 838. <http://dx.doi.org/10.1007/s11082-024-06370-2>
22. A. Iftikhar, A. Ghafoor, T. Zubair, S. Firdous, S. Mohyud-Din, $(G'/G, 1/G)$ -expansion method for traveling wave solutions of $(2+1)$ dimensional generalized KdV, Sin Gordon and Landau-Ginzburg-Higgs equations, *Sci. Res. Essays*, **8** (2013), 1349–1359. <http://dx.doi.org/10.5897/SRE2013.5555>
23. R. Ali, S. Barak, A. Altalbe, Analytical study of soliton dynamics in the realm of fractional extended shallow water wave equations, *Phys. Scr.*, **99** (2024), 065235. <http://dx.doi.org/10.1088/1402-4896/ad4784>
24. M. Bhatti, D. Lu, An application of Nwogu Boussinesq model to analyze the head-on collision process between hydroelastic solitary waves, *Open Phys.*, **17** (2019), 177–191. <http://dx.doi.org/10.1515/phys-2019-0018>
25. S. Behera, N. Aljahdaly, Nonlinear evolution equations and their traveling wave solutions in fluid media by modified analytical method, *Pramana*, **97** (2023), 130. <http://dx.doi.org/10.1007/s12043-023-02602-4>
26. H. Khan, S. Barak, P. Kumam, M. Arif, Analytical solutions of fractional Klein-Gordon and gas dynamics equations, via the (G'/G) -expansion method, *Symmetry*, **11** (2019), 566. <http://dx.doi.org/10.3390/sym11040566>
27. J. He, X. Wu, Exp-function method for nonlinear wave equations, *Chaos Soliton. Fract.*, **30** (2006), 700–708. <http://dx.doi.org/10.1016/j.chaos.2006.03.020>
28. A. Alharbi, M. Almatrafi, Riccati-Bernoulli sub-ODE approach on the partial differential equations and applications, *Int. J. Math. Comput. Sci.*, **15** (2020), 367–388.
29. W. Thadee, A. Chankaew, S. Phoosree, Effects of wave solutions on shallow-water equation, optical-fibre equation and electric-circuit equation, *Maejo Int. J. Sci. Tech.*, **16** (2022), 262–274.
30. J. Alzaidy, Fractional sub-equation method and its applications to the space-time fractional differential equations in mathematical physics, *British Journal of Mathematics and Computer Science*, **3** (2013), 153–163. <http://dx.doi.org/10.9734/BJMCS/2013/2908>
31. M. Cinar, A. Secer, M. Ozisik, M. Bayram, Derivation of optical solitons of dimensionless Fokas-Lenells equation with perturbation term using Sardar sub-equation method, *Opt. Quant. Electron.*, **54** (2022), 402. <http://dx.doi.org/10.1007/s11082-022-03819-0>
32. K. J. Wang, F. Shi, Multi-soliton solutions and soliton molecules of the $(2+1)$ -dimensional Boiti-Leon-Manna-Pempinelli equation for the incompressible fluid, *EPL*, **145** (2024), 42001. <http://dx.doi.org/10.1209/0295-5075/ad219d>

33. M. Alqhtani, K. Saad, R. Shah, W. Hamanah, Discovering novel soliton solutions for (3+1)-modified fractional Zakharov-Kuznetsov equation in electrical engineering through an analytical approach, *Opt. Quant. Electron.*, **55** (2023), 1149. <http://dx.doi.org/10.1007/s11082-023-05407-2>
34. H. Yasmin, N. Aljahdaly, A. Saeed, R. Shah, Probing families of optical soliton solutions in fractional perturbed Radhakrishnan Kundu Lakshmanan model with improved versions of extended direct algebraic method, *Fractal Fract.*, **7** (2023), 512. <http://dx.doi.org/10.3390/fractalfract7070512>
35. M. Mossa Al-Sawalha, H. Yasmin, R. Shah, A. Ganie, K. Moaddy, Unraveling the dynamics of singular stochastic solitons in stochastic fractional Kuramoto-Sivashinsky equation, *Fractal Fract.*, **7** (2023), 753. <http://dx.doi.org/10.3390/fractalfract7100753>
36. H. Yasmin, N. Aljahdaly, A. Saeed, R. Shah, Investigating families of soliton solutions for the complex structured coupled fractional Biswas-Arshed model in birefringent fibers using a novel analytical technique, *Fractal Fract.*, **7** (2023), 491. <http://dx.doi.org/10.3390/fractalfract7070491>
37. W. Gao, P. Veerasha, D. Prakasha, H. Baskonus, G. Yel, New numerical results for the time-fractional Phi-four equation using a novel analytical approach, *Symmetry*, **12** (2020), 478. <http://dx.doi.org/10.3390/sym12030478>
38. H. Rezazadeh, H. Tariq, M. Eslami, M. Mirzazadeh, Q. Zhou, New exact solutions of nonlinear conformable time-fractional Phi-4 equation, *Chinese J. Phys.*, **56** (2018), 2805–2816. <http://dx.doi.org/10.1016/j.cjph.2018.08.001>
39. M. Khater, A. Mousa, M. El-Shorbagy, R. Attia, Analytical and semi-analytical solutions for Phi-four equation through three recent schemes, *Results Phys.*, **22** (2021), 103954. <http://dx.doi.org/10.1016/j.rinp.2021.103954>
40. Z. Li, T. Han, C. Huang, Bifurcation and new exact traveling wave solutions for time-space fractional Phi-4 equation, *AIP Adv.*, **10** (2020), 115113. <http://dx.doi.org/10.1063/5.0029159>
41. S. Bibi, N. Ahmed, U. Khan, S. Mohyud-Din, Auxiliary equation method for ill-posed Boussinesq equation, *Phys. Scr.*, **94** (2019), 085213. <http://dx.doi.org/10.1088/1402-4896/ab1951>
42. M. Abdelrahman, H. Alkhidhr, Closed-form solutions to the conformable space-time fractional simplified MCH equation and time fractional Phi-4 equation, *Results Phys.*, **18** (2020), 103294. <http://dx.doi.org/10.1016/j.rinp.2020.103294>
43. F. Mahmud, M. Samsuzzoha, M. Ali Akbar, The generalized Kudryashov method to obtain exact traveling wave solutions of the PHI-four equation and the Fisher equation, *Results Phys.*, **7** (2017), 4296–4302. <http://dx.doi.org/10.1016/j.rinp.2017.10.049>
44. M. Younis, A. Zafar, The modified simple equation method for solving nonlinear Phi-Four equation, *International Journal of Innovation and Applied Studies*, **2** (2013), 661–664.
45. P. Sunthrayuth, N. Aljahdaly, A. Ali, R. Shah, I. Mahariq, A. Tchalla, ϕ -Haar wavelet operational matrix method for fractional relaxation-oscillation equations containing ϕ -Caputo fractional derivative, *J. Funct. Space.*, **2021** (2021), 7117064. <http://dx.doi.org/10.1155/2021/7117064>

46. S. Noor, H. Alyousef, A. Shafee, R. Shah, S. El-Tantawy, A novel analytical technique for analyzing the (3+1)-dimensional fractional calogero-bogoyavlenskii-schiff equation: investigating solitary/shock waves and many others physical phenomena, *Phys. Scr.*, **99** (2024), 065257. <http://dx.doi.org/10.1088/1402-4896/ad49d9>
47. S. Noor, A. Alshehry, A. Shafee, R. Shah, Families of propagating soliton solutions for (3+1)-fractional Wazwaz-BenjaminBona-Mahony equation through a novel modification of modified extended direct algebraic method, *Phys. Scr.*, **99** (2024), 045230. <http://dx.doi.org/10.1088/1402-4896/ad23b0>
48. H. Yasmin, A. Alshehry, A. Ganie, A. Mahnashi, R. Shah, Perturbed Gerdjikov-Ivanov equation: soliton solutions via Backlund transformation, *Optik*, **298** (2024), 171576. <http://dx.doi.org/10.1016/j.ijleo.2023.171576>
49. S. El-Tantawy, H. Alyousef, R. Matoog, R. Shah, On the optical soliton solutions to the fractional complex structured (1+1)-dimensional perturbed gerdjikov-ivanov equation, *Phys. Scr.*, **99** (2024), 035249. <http://dx.doi.org/10.1088/1402-4896/ad241b>
50. S. Alshammari, K. Moaddy, R. Shah, M. Alshammari, Z. Alsheekhussain, M. Mossa Al-sawalha, et al., Analysis of solitary wave solutions in the fractional-order Kundu-Eckhaus system, *Sci. Rep.*, **14** (2024), 3688. <http://dx.doi.org/10.1038/s41598-024-53330-7>
51. H. Yasmin, A. Alshehry, A. Ganie, A. Shafee, R. Shah, Noise effect on soliton phenomena in fractional stochastic Kraenkel-Manna-Merle system arising in ferromagnetic materials, *Sci. Rep.*, **14** (2024), 1810. <http://dx.doi.org/10.1038/s41598-024-52211-3>



AIMS Press

©2024 the Author(s), licensee AIMS Press. This is an open access article distributed under the terms of the Creative Commons Attribution License (<https://creativecommons.org/licenses/by/4.0>)